



ELSEVIER

Available online at www.sciencedirect.com

SCIENCE @ DIRECT®

Journal of Sound and Vibration 284 (2005) 227–248

JOURNAL OF
SOUND AND
VIBRATION

www.elsevier.com/locate/jsvi

Propagation characteristics of Rayleigh waves in transversely isotropic piezothermoelastic materials

J.N. Sharma^{a,*}, Mohinder Pal^b, Dayal Chand^c

^a*Department of Applied Sciences, National Institute of Technology, Hamirpur (HP) 177005, India*

^b*Department of Physics, Institute of Engineering & Technology, Baddal, Punjab 141001, India*

^c*Department of Physics, Beant College of Engineering & Technology, Gurdaspur 143521, India*

Received 17 October 2003; received in revised form 13 April 2004; accepted 14 June 2004

Available online 21 November 2004

Abstract

The paper is aimed at to investigate the propagation of Rayleigh waves in a homogeneous, transversely isotropic, piezothermoelastic half-space subjected to stress free, electrically shorted/charge-free and thermally insulated/isothermal boundary conditions. Secular equations for the half-space in closed form and isolated mathematical conditions in completely separate terms are derived. The secular equations for stress free piezoelectric, thermoelastic and elastic half-spaces have also been deduced as special cases from the present analysis. Finally, numerical solution of various secular equations and other relevant relations is carried out for cadmium-selenide (6 mm class) material. The dispersion curves and attenuation coefficients of wave propagation are presented graphically, in order to illustrate and compare the analytical results. The theory and numerical computations are found to be in close agreement. The coupling between the thermal/electric/elastic fields in piezoelectric materials provides a mechanism for sensing thermomechanical disturbances from measurements of induced electric potentials, and for altering structural responses via applied electric fields. Therefore, the analysis will be useful in the design and construction of temperature sensors and surface acoustic wave filter devices.

© 2004 Elsevier Ltd. All rights reserved.

*Corresponding author. Tel.: +91 1972 223296; fax: +91 1972 223834.

E-mail address: jns@recham.ernet.in (J.N. Sharma).

1. Introduction

The theory of thermo-piezoelectricity was first proposed by Mindlin [1]. He also derived governing equations of a thermo-piezoelectric plate [2]. The physical laws for the thermo-piezoelectric materials have been explored by Nowacki [3–5]. Chandrasekharaiah [6,7] has generalized Mindlin's theory of thermo-piezoelectricity to account for the finite speed of propagation of thermal disturbances. Several investigators [8–11] have studied the propagation of waves in plates, cylinders and general three-dimensional bodies that are made of thermo-piezoelectric materials. The propagation of plane harmonic waves in anisotropic thermoelastic materials have been discussed by many authors [11–15]. The propagation of surface waves in homogeneous thermoelastic media has been discussed by Chadwick [17] and Nayfeh and Nasser [18]. Chadwick and Windle [19] studied the effect of heat conduction upon the propagation of Rayleigh waves in the semi-infinite elastic solid (i) when the surface of solid is maintained at constant temperature and (ii) when the surface is thermally insulated. Chadwick and Atkin [20] corrected and extended the earlier work of Chadwick and Windle [19] by reconsidering the same problem. Sharma and Singh [21] studied thermoelastic surface waves in a transversely isotropic half-space. Yang and Batra [22] studied the effect of heat conduction on shift in the frequencies of a freely vibrating linear piezoelectric body with the help of two perturbation methods. It is shown that the first-order effect on frequencies is to shift them by a small imaginary number thereby signifying that the effect of energy dissipation due to heat conduction is to reduce the amplitude of vibration. Sharma and Kumar [23] have studied the propagation of plane harmonic waves in piezothermoelastic materials. Sharma and Pal [24,25] studied the propagation of Lamb waves in infinite piezoelectric elastic plate and Rayleigh Lamb waves in magneto-thermoelastic homogeneous isotropic plate. The wave propagation in elastic solid has been treated extensively in detail by Graff [26] and Achenbach [27].

In pure solid half-space, the discovery of Rayleigh waves is tightly connected with the earthquake spectrum analysis [28]. Owing to the slower attenuation of energy than that of the body waves and the characteristics that it propagates along the surface, Rayleigh waves cause destructive vibration to the structures. However, due to nonlinearity, it is difficult to get the exact solution of the characteristic equation of Rayleigh waves in anisotropic media. As a result, though many researches [29–32] have been carried out on the propagation of Rayleigh waves in anisotropic solids. No problem, which analyses the propagation of surface waves in piezothermoelastic half-space analytically, is available in the literature as per the knowledge of authors. Recently, thermoelastic wave propagation has been studied by Sharma et al. [33] and Sharma [34] in infinite piezothermoelastic media and plates. The coupling between the thermal/electric/elastic fields in piezoelectric materials provides a mechanism for sensing thermomechanical disturbances from measurements of induced electric potentials, and for altering structural responses via applied electric fields. In view of this phenomenon, an attempt has been made in the present paper to investigate the propagation of Rayleigh waves in piezothermoelastic, transversely isotropic half-space that is subjected to stress free, thermally insulated/isothermal and electrically shorted/charge free boundary conditions. The analytical results have been verified and computed numerically for cadmium-selenide (CdSe) material plate, which are found to be in close agreement with the analytical results.

2. Basic equations

The equations governing linear piezoelectric thermoelastic interactions in homogeneous anisotropic solid are [23]

(A) Strain–displacement relations:

$$S_{ij} = \frac{1}{2}(u_{i,j} + u_{j,i}), \quad i, j = 1, 2, 3. \tag{1}$$

(B) Stress–strain–temperature and electric field relations:

$$\sigma_{ij} = c_{ijkl}S_{kl} - \beta_{ij}T - e_{kij}E_k, \quad i, j, k, l = 1, 2, 3. \tag{2}$$

(C) Equation of motion:

$$\sigma_{ij,j} + \rho F_i = \rho \ddot{u}_i, \quad i, j = 1, 2, 3. \tag{3}$$

(D) Heat conduction equation:

$$K_{ij}T_{,ij} = T_0(\beta_{ij}\dot{u}_{i,j} - p_i\dot{\phi}_{,i}) + \rho C_e \dot{T}, \quad i, j = 1, 2, 3. \tag{4}$$

(E) Gauss equation:

$$D_{i,i} = 0, \quad D_i = e_{ijk}S_{jk} + \epsilon_{ij}E_j + p_iT, \quad i, j, k = 1, 2, 3, \tag{5}$$

where $E_i = -\phi_{,i}$ is the electric field and D_i the electric displacement.

In Eqs. (1)–(5), ρ is the mass density, u_i the mechanical displacement, S_{ij} the strain tensor, σ_{ij} the stress tensor, T the temperature change of a material particle, T_0 the reference uniform temperature of the body, K_{ij} the heat conduction tensor, c_{ijkl} the isothermal elastic parameters tensor, e_{kij} the piezoelectric moduli, β_{ij} the thermal elastic coupling tensor, ϵ_{ij} the electric permittivity, C_e the specific heat at constant strain and p_i are the pyroelectric moduli. The comma notation is used for spatial derivatives and superimposed dot represent time differentiation.

These parameters are assumed to satisfy the following conditions:

- (i) The thermal conductivity K_{ij} and electric permittivity ϵ_{ij} are symmetric and positive definite.
- (ii) The thermoelastic coupling tensor β_{ij} is non-singular.
- (iii) The specific heat C_e at constant strain is positive.
- (iv) The isothermal linear elasticities are positive definite in the sense that $c_{ijkl}S_{ij}S_{kl} \geq 0$.
- (v) The piezoelectric moduli tensor e_{kij} is symmetric with respect to i and j and pyroelectric moduli p_i is positive.

3. Formulation of the problem

We consider homogeneous transversely isotropic, thermally and electrically conducting piezoelectric medium in the undeformed state at uniform temperature T_0 and initial potential ϕ_0 . We assume that medium is transversely isotropic in such a way that planes of isotropy are perpendicular to x_3 -axis. We take origin of the coordinate system (x_1, x_2, x_3) at any point on the plane surface and x_3 -axis pointing vertically downward into the half-space, which is thus represented by $x_3 \geq 0$. We assume that surface $x_3 = 0$ is stress free, thermally insulated/isothermal

and electrically shorted/charge free. We chose x_1 -axis in the direction of wave propagation so that all particles on a line parallel to x_2 -axis are equally displaced. Therefore, all the field quantities will be independent of x_2 coordinate. Further the disturbance is assumed to be confined to the neighbourhood of the free surface $x_3=0$ and hence vanishes as $x_3 \rightarrow \infty$. In linear theory of homogeneous, transversely isotropic, coupled piezothermoelasticity, the basic governing field Eqs. (3)–(5) for temperature change $T(x_1, x_3, t)$, displacement vector $\vec{u}(x_1, x_3, t) = (u_1, 0, u_3)$ and electric potential $\phi(x_1, x_3, t)$, in the absence of charge density, heat sources and body forces, are given by

$$c_{11}u_{1,11} + c_{44}u_{1,13} + (c_{13} + c_{44})u_{3,13} + (e_{15} + e_{31})\phi_{,13} - \beta_1 T_{,1} = \rho \ddot{u}_1, \quad (6)$$

$$(c_{13} + c_{44})u_{1,13} + c_{44}u_{3,11} + c_{33}u_{3,33} + e_{15}\phi_{,11} + e_{33}\phi_{,33} - \beta_3 T_{,3} = \rho \ddot{u}_3, \quad (7)$$

$$(e_{15} + e_{31})u_{1,13} + e_{15}u_{3,11} + e_{33}u_{3,33} - \epsilon_{11}\phi_{,11} - \epsilon_{33}\phi_{,33} + p_3 T_{,3} = 0, \quad (8)$$

$$K_{11}T_{,11} + K_{33}T_{,33} - \rho c_e \dot{T} = T_0[\beta_1 \dot{u}_{1,1} + \beta_3 \dot{u}_{3,3} - p_3 \dot{\phi}_{,3}], \quad (9)$$

where $\beta_1 = (c_{11} + c_{12})\alpha_1 + c_{13}\alpha_3$, $\beta_3 = 2c_{13}\alpha_1 + c_{33}\alpha_3$; α_1 , α_3 and K_{11} , K_{33} are, respectively, the coefficients of linear thermal expansion and thermal conductivity, in the direction orthogonal to axes of symmetry and along the axis of symmetry; ρ , and C_e are, respectively, the mass density and specific heat at constant strain, c_{ij} are the isothermal elastic parameters, e_{ij} are the piezoelectric constants, ϵ_{11} and ϵ_{33} are electric permittivities and p_3 is pyroelectric constant. We define the quantities

$$\begin{aligned} x'_i &= \frac{\omega^* x_i}{v_p}, & t' &= \omega^* t, & u'_i &= \frac{\rho \omega^* v_p u_i}{\beta_1 T_0}, & T' &= \frac{T}{T_0}, & \phi' &= \frac{\phi}{\phi_0}, & \omega^* &= \frac{C_e c_{11}}{K_{11}}, & \epsilon &= \frac{T_0 \beta_1^2}{\rho C_e c_{11}}, \\ v_p &= \sqrt{\frac{c_{11}}{\rho}}, & p &= \frac{p_3 c_{11}}{\beta_1 e_{33}}, & c_1 &= \frac{c_{33}}{c_{11}}, & c_2 &= \frac{c_{44}}{c_{11}}, & c_3 &= \frac{c_{13} + c_{44}}{c_{11}}, & c_4 &= \frac{c_{11} - c_{12}}{2c_{11}}, \\ e_1 &= \frac{e_{15} + e_{31}}{e_{33}}, & e_2 &= \frac{e_{15}}{e_{33}}, & \bar{\epsilon} &= \frac{\epsilon_{11}}{\epsilon_{33}}, & \epsilon_p &= \frac{\omega^* e_{33} \phi_0}{v_p \beta_1 T_0}, & \epsilon_\eta &= \eta_3 \epsilon_p, & \eta_3 &= \frac{\epsilon_{33} c_{11}}{e_{33}^2}, \\ \omega' &= \frac{\omega}{\omega^*}, & c' &= \frac{c}{v_p}, & d' &= \frac{\omega^* d}{v_p}, & h' &= \frac{h v_p}{\omega^*}, & \zeta' &= \frac{\zeta v_p}{\omega^*}, & \sigma'_{ij} &= \frac{\sigma_{ij}}{\beta_1 T_0}, & \bar{\beta} &= \frac{\beta_3}{\beta_1}, \\ \bar{K} &= \frac{K_{33}}{K_{11}}, & D'_i &= \frac{D_i}{\beta_1 T_0}. \end{aligned} \quad (10)$$

Here ϵ is the thermo-elastic coupling constant, ω^* is the characteristic frequency of the medium, ϵ_p is the piezothermoelastic coupling constant and v_p is the longitudinal wave velocity in the medium. Upon introducing the quantities (10) in Eqs. (6)–(9), we obtain

$$\begin{aligned} u_{1,11} + c_2 u_{1,33} + c_3 u_{3,13} + \epsilon_p e_1 \phi_{,13} - T_{,1} &= \ddot{u}_1, \\ c_3 u_{1,13} + c_2 u_{3,11} + c_1 u_{3,33} + \epsilon_p (e_2 \phi_{,11} + \phi_{,33}) - \bar{\beta} T_{,3} &= \ddot{u}_3, \\ e_1 u_{1,13} + e_2 u_{3,11} + u_{3,33} - \epsilon_\eta (\bar{\epsilon} \phi_{,11} + \phi_{,33}) + p T_{,3} &= 0, \\ T_{,11} + \bar{K} T_{,33} - \dot{T} &= \epsilon [\dot{u}_{1,1} + \bar{\beta} \dot{u}_{3,3} - \epsilon_p p \dot{\phi}_{,3}]. \end{aligned} \quad (11)$$

Here primes have been suppressed for convenience.

The non-dimensional form of stresses and electric displacement components given by Eqs. (2) and (5) in x_1-x_3 plane, are given by

$$\begin{aligned} \sigma_{11} &= u_{1,1} + (1 - 2c_4)u_{2,2} + (c_3 - c_2)u_{3,3} + (e_1 - e_2)\phi_{,3} - T, \\ \sigma_{33} &= (c_3 - c_2)u_{1,1} + c_1u_{3,3} + \epsilon_p\phi_{,3} - \bar{\beta}T, \\ \sigma_{13} &= c_2(u_{1,3} + u_{3,1}) + \epsilon_p e_2\phi_{,1}, \\ D_1 &= e_2(u_{1,3} + u_{3,1}) - \epsilon_\eta\phi_{,1} \\ D_3 &= (e_1 - e_2)u_{1,1} + u_{3,3} - \epsilon_\eta\phi_{,3} + pT. \end{aligned} \tag{12}$$

3.1. Boundary conditions

In order to study the effect of heat dissipation on propagation of waves due to coupling between thermoelastic and pyroelectric fields, the surface $x_3 = 0$ of the half-space is assumed to be stress free, thermally insulated/isothermal and electrically shorted/charge free. Then the non-dimensional boundary conditions at the surface $x_3 = 0$ of the material are given as below:

(i) *Mechanical conditions* (stress free surfaces): Because the surface of half-space is assumed to be stress free so that

$$\sigma_{33} = (c_3 - c_2)u_{1,1} + c_1u_{3,3} + \epsilon_p\phi_{,3} - \bar{\beta}T = 0, \tag{13.1}$$

$$\sigma_{13} = c_2(u_{1,3} + u_{3,1}) + \epsilon_p e_2\phi_{,1} = 0. \tag{13.2}$$

(ii) *Thermal conditions*: The surface of half-space is subjected to thermally insulated or isothermal conditions, which leads to

$$T_{,3} + hT = 0, \tag{13.3}$$

where h is the surface heat transfer coefficient. Here $h \rightarrow 0$ corresponds to thermally insulated surface and $h \rightarrow \infty$ refers to isothermal one.

(iii) *Electrical conditions*: The surface of half-space is either electrically shorted or maintained at charge free conditions which respectively, implies that

$$\phi = 0, \tag{13.4a}$$

$$D_3 = (e_1 - e_2)u_{1,1} + u_{3,3} - \epsilon_\eta\phi_{,3} + pT = 0. \tag{13.4b}$$

4. Formal solution

We assume solution of the form

$$(u_1, u_3, \phi, T) = (1, V, W, S,)Ue^{i\xi(x_1 \sin \theta + mx_3 - ct)}, \tag{14}$$

where ξ is the wavenumber, ω is the angular frequency and $c = (\omega/\xi)$ is the phase velocity of the wave. Here θ is the angle of inclination of wave normal with axes of symmetry (x_3 -axis), m is an

unknown parameter, V , W and S are, respectively, the amplitude ratios of displacement u_3 , electric potential ϕ and temperature change T to that of displacement component u_1 . The use of Eq. (14) in Eqs. (11) leads to a system of following coupled equations in terms of the amplitudes $[1, V, W, S]^T$. We have

$$\begin{bmatrix} s^2 + c_2m^2 - c^2 & c_3ms & \epsilon_p e_1ms & -s \\ c_3ms & c_2s^2 + c_1m^2 - c^2 & \epsilon_p(e_2s^2 + m^2) & -\bar{\beta}m \\ e_1ms & e_2s^2 + m^2 & -\epsilon_\eta(\bar{\epsilon}s^2 + m^2) & pm \\ c^2 \in s & c^2 \in \bar{\beta}m & -c^2 \in \epsilon_p pm & c^2 + z(s^2 + \bar{K}m^2) \end{bmatrix} \begin{bmatrix} 1 \\ V \\ W \\ S \end{bmatrix} = \begin{bmatrix} 0 \\ 0 \\ 0 \\ 0 \end{bmatrix}, \quad (15)$$

where $z = i\omega$, $s = \sin \theta$. The system of Eqs. (15) has a non-trivial solution if the determinant of coefficients of $[1, V, W, S]^T$ vanishes which leads to following polynomial characteristic equation

$$m^8 + \left(a_1 + \frac{s^2}{\bar{K}} + \frac{Fc^2}{z\bar{K}} \right) m^6 + \left(a_2 + a_1 \frac{s^2}{\bar{K}} + \frac{Fc^2}{\bar{K}z} A_1 \right) m^4 + \left(a_3 + a_2 \frac{s^2}{\bar{K}} + \frac{Fc^2}{\bar{K}z} A_2 \right) m^2 + \left(a_3 \frac{s^2}{\bar{K}} + \frac{Fc^2 A_3}{\bar{K}z} \right) = 0, \quad (16)$$

where the coefficients a_i and A_i , $i = 1, 2, 3$ are defined in Appendix A. The characteristic equation (16) is biquadratic in m^2 and hence possesses four roots m_i^2 , $i = 1, 2, 3, 4$. Since, we are interested in surface waves only so it is essential that motion is confined to free surface $x_3 = 0$ of the half-space so that the characteristic roots m_i^2 must satisfy the radiation condition $\text{Im}(m_i) \geq 0$. Then the formal solution for displacements, temperature change and electric potential is written as

$$(u_1, u_3, \phi, T) = \sum_{q=1}^4 (1, V_q, W_q, S_q) U_q \exp\{i\zeta(x_1 \sin \theta - m_q x_3 - ct)\}. \quad (17)$$

The amplitude ratios V , W , and S for each m_q , $q = 1, 2, 3, 4$ can be expressed as

$$V_q = R_1(m_q)/R(m_q), \quad W_q = R_2(m_q)/R(m_q), \quad S_q = R_3(m_q)/R(m_q), \quad (18)$$

where $R(m_q)$ and $R_i(m_q)$, $i = 1, 2, 3$ are given in Appendix A.

Upon using Eq. (17) in the constitutive relation (12), the stresses, electric displacement and temperature gradient, are obtained as

$$(\sigma_{33}, \sigma_{13}, D_3, T_{,3}) = \sum_{q=1}^4 i\zeta (D_{1q}, D_{2q}, D_{3q}, m_q S_q) U_q \exp\{i\zeta(x_1 \sin \theta - m_q x_3 - ct)\}, \quad (19)$$

where

$$D_{1q} = (c_3 - c_2) \sin \theta + c_1 m_q V_q + \epsilon_p m_q W_q - \frac{\bar{\beta}}{i\zeta} S_q, \quad (20.1)$$

$$D_{2q} = c_2 m_q + c_2 \sin \theta V_q + \epsilon_p e_2 \sin \theta W_q, \quad (20.2)$$

$$D_{3q} = (e_1 - e_2) \sin \theta + m_q V_q - \epsilon_\eta m_q W_q + p S_q / i\zeta, \quad q = 1, 2, 3, 4. \quad (20.3)$$

5. Derivation of the secular equations

5.1. Stress and charge free surface of the half-space

By invoking stress free, isothermal and charge free boundary conditions (13.1)–(13.4) at the surface $x_3=0$, we obtain a system of eight simultaneous linear equations in amplitudes U_q , $q = 1, 2, 3, 4$ as

$$\sum_{q=1}^4 D_{1q}U_q = 0, \quad \sum_{q=1}^4 D_{2q}U_q = 0, \quad \sum_{q=1}^4 D_{3q}U_q = 0, \quad \sum_{q=1}^4 D_{4q}U_q = 0, \quad (21)$$

where $D_{4q} = (m_q + h)S_q$, $q = 1, 2, 3, 4$.

The system of Eqs. (21) has a non-trivial solution if the determinant of the coefficients of U_q , $q = 1, 2, 3, 4$ vanishes, which after applying algebraic reductions and manipulations, leads to a characteristic equation for the propagation of modified guided waves in the piezothermoelastic half-space. The corresponding secular equation is obtained as below:

$$D_{41}G_1 - D_{42}G_2 + D_{43}G_3 - D_{44}G_4 = 0, \quad (22)$$

$$G_1 = \begin{vmatrix} D_{12} & D_{13} & D_{14} \\ D_{22} & D_{23} & D_{24} \\ D_{32} & D_{33} & D_{34} \end{vmatrix}, \quad G_2 = \begin{vmatrix} D_{11} & D_{13} & D_{14} \\ D_{21} & D_{23} & D_{24} \\ D_{31} & D_{33} & D_{34} \end{vmatrix},$$

$$G_3 = \begin{vmatrix} D_{11} & D_{12} & D_{14} \\ D_{21} & D_{22} & D_{24} \\ D_{31} & D_{32} & D_{34} \end{vmatrix}, \quad G_4 = \begin{vmatrix} D_{11} & D_{12} & D_{13} \\ D_{21} & D_{22} & D_{23} \\ D_{31} & D_{32} & D_{33} \end{vmatrix}. \quad (23)$$

For thermally insulated ($h \rightarrow 0$) piezothermoelastic half-space, the secular equation (22) becomes

$$m_1S_1G_1 - m_2S_2G_2 + m_3S_3G_3 - m_4S_4G_4 = 0. \quad (24)$$

Eq. (22) in case of isothermal ($h \rightarrow \infty$) piezothermoelastic half-space reduces to

$$S_1G_1 - S_2G_2 + S_3G_3 - S_4G_4 = 0. \quad (25)$$

5.2. Stress free and electrically shorted surfaces of the half-space

Upon invoking the stress free, thermally insulated and electrically shorted boundary conditions (13.1)–(13.4) at the surface $x_3 = 0$, we obtain

$$D_{41}G'_1 - D_{42}G'_2 + D_{43}G'_3 - D_{44}G'_4 = 0, \quad (26)$$

where $D_{4q} = (m_q + h)S_q$ and G'_1, G'_2, G'_3, G'_4 are obtained from G_i , $i = 1, 2, 3, 4$ by replacing D_{3q} with W_q in Eq. (23). The secular equation (26) in case of thermally insulated ($h \rightarrow 0$) and

isothermal ($h \rightarrow \infty$) surfaces of the half-space, reduce to

$$m_1 S_1 G'_1 - m_2 S_2 G'_2 + m_3 S_3 G'_3 - m_4 S_4 G'_4 = 0, \quad (27)$$

$$S_1 G'_1 - S_2 G'_2 + S_3 G'_3 - S_4 G'_4 = 0, \quad (28)$$

respectively. The secular equations (24)–(28) contain complete information about the phase velocity, wavenumber and attenuation coefficient of the surface waves in a piezothermoelastic half-space. In general, wavenumber and hence the phase velocities of the waves are complex quantities, therefore the waves are attenuated in space. If we write

$$c^{-1} = V^{-1} + i\omega^{-1}Q, \quad (29)$$

so that $\xi = R + iQ$, where $R = \omega/V$ and V, Q are real numbers. Also the roots of characteristic equation (16) are, in general complex, and hence we assume that $m_q = \alpha_q + i\beta_q$, so that the exponent in the plane wave solution (17) becomes

$$-R \left\{ \frac{Q}{R} x_1 \sin \theta + m_q^I x_3 \right\} - iR \{ x_1 \sin \theta - m_q^R x_3 - Vt \},$$

where $m_q^R = \alpha_q - \beta_q Q/R$, $m_q^I = \beta_q + \alpha_q Q/R$. This shows that V is the propagation velocity and Q is the attenuation coefficient of the wave. Upon using representation (29) in secular equations (23)–(28), the values of propagation speed V and attenuation coefficient Q for different modes of wave propagation can be obtained. Since $c' = c/V_p$ is the non-dimensional complex phase velocity, so $V' = V/V_p$ and $Q' = V_p Q$ are the non-dimensional phase speed and attenuation coefficient, respectively. Here dashes have been omitted for convenience. Eq. (17) can be rewritten as

$$(u_1, u_3, \phi, T) = (1, V_q, W_q, S_q) U \exp\{-Qx_1 \sin \theta - k_q^I x_3\} \exp\{i[k_q^R x_3 - R(x_1 \sin \theta - Vt)]\} \quad (30)$$

with $k_q = R(m_q^R + im_q^I) = k_q^R + ik_q^I$ (say). From Eq. (30) it can be obtained that the disturbance direction of Rayleigh wave inclines to the free surface with the angle of $\theta = \cos^{-1}(m_q^R)$. Moreover, it is apparent that

$$|k_q^R|^2 - |k_q^I|^2 = R^2 \{(m_q^R)^2 - (m_q^I)^2\}, \quad |k_q^R| |k_q^I| \cos \delta = \frac{1}{2} R^2 m_q^R m_q^I.$$

As shown in Fig. 1, the phase plane (the plane vertical to vector k_q^R) and the amplitude plane (the plane vertical to vector k_q^I) are not parallel to each other any more. Therefore, the maximum attenuation is not along the direction of wave propagation but along the direction of vector k_q^I .

6. Special cases

6.1. Uncoupled thermoelasticity (piezoelectric half-space)

If we set $\epsilon = 0 = p$, the motion corresponding to thermal wave (T-mode) decouples from rest of the motion and the various results reduce to those of stress free piezoelectric elastic half-space. The secular equations for charge free and electrically shorted surface of half-space are,

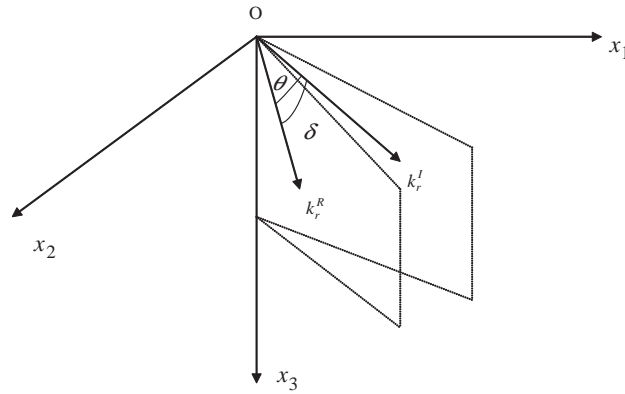


Fig. 1. Complex wave vector of Rayleigh waves in piezothermoelastic media.

respectively, given as

$$D'_{31}F_1 - D'_{32}F_2 + D'_{33}F_3 = 0, \tag{31}$$

$$W'_1F_1 - W'_2F_2 + W''_3F_3 = 0, \tag{32}$$

where

$$F_1 = D'_{12}D'_{23} - D'_{22}D'_{13}, \quad F_2 = D'_{11}D'_{23} - D'_{21}D'_{13}, \quad F_3 = D'_{11}D'_{22} - D'_{21}D'_{12},$$

$$D'_{1q} = (c_3 - c_2) \sin \theta + c_1 m_q V'_q + m_q W'_q,$$

$$D'_{2q} = c_2 m_q + c_2 \sin \theta V'_q + e_2 \sin \theta W'_q,$$

$$V'_q = -R'_1(m_q)/R'(m_q), \quad W'_q = R'_2(m_q)/R'(m_q),$$

$$R'_1(m_q) = [c_2 e_3 m_q^4 + \{(e_3 + c_2 e_2 - e_1 c_3) s^2 - e_3 c^2\} m_q^2 + e_2 s^2 (s^2 - c^2)],$$

$$R'_2(m_q) = c_1 c_2 m_q^4 + (P s^2 - J c^2) m_q^2 + (s^2 - c^2)(c_2 s^2 - c^2), \tag{33}$$

$$R'(m_q) = m_q s [(c_3 e_3 - c_1 e_1) m_q^2 + (c_3 e_2 - e_1 c_2) s^2 + e_1 c^2].$$

Here $m_q, q = 1, 2, 3$ are the roots of the equation

$$m^6 + a_1 m^4 + a_2 m^2 + a_3 = 0, \tag{34}$$

where a_1, a_2, a_3 are defined in Appendix A.

6.2. Stress free thermoelastic half-space

In the absence of piezoelectric effect, we have $\epsilon_P = 0 = p$, the various results reduce to those of stress free thermoelastic plate. The secular equation (22) for isothermal and thermally insulated

surface of half-space in this case becomes

$$D''_{41}F'_1 - D''_{42}F'_2 + D''_{44}F'_4 = 0, \tag{35}$$

where

$$\begin{aligned} F'_1 &= D''_{12}D''_{24} - D''_{22}D''_{14}, & F'_2 &= D''_{11}D''_{24} - D''_{21}D''_{14}, & F'_4 &= D''_{11}D''_{22} - D''_{21}D''_{12}, \\ D''_{1q} &= (c_3 - c_2) \sin \theta + c_1 m_q V_q^* - \bar{\beta} S_q / i \xi, \\ D''_{2q} &= c_2 m_q + c_2 \sin \theta V_q^*, \\ D''_{4q} &= \begin{cases} S_q^*, & \text{for isothermal,} \\ m_q S_q^*, & \text{for thermally insulated,} \end{cases} \end{aligned} \tag{36}$$

$$\begin{aligned} V_q^* &= \begin{cases} m_q \alpha_q / \sin \theta, & q = 1, 2, \\ -(c_2 m_q^2 + \sin^2 \theta - c^2 + c_3 \sin \theta S_q^*) / c_3 m_q \sin \theta, & q = 4, \end{cases} \\ S_q^* &= \begin{cases} [(c_2 + c_3 \alpha_q) m_q^2 + s^2 - c^2] / s, & q = 1, 2, \\ \frac{[(c_1 m_q^2 + c_2 \sin^2 \theta - c^2)(c_2 m_q^2 + \sin^2 \theta - c^2) - c_3^2 m_q^2 \sin^2 \theta]}{\sin \theta [(c_1 - c_3 \bar{\beta}) m_q^2 + c_2 \sin^2 \theta - c^2]}, & q = 4, \end{cases} \\ \alpha_q &= \bar{\beta} \frac{[c_2 m_q^2 + (1 - c_3 / \bar{\beta}) s^2 - c^2]}{(c_1 - c_3 \bar{\beta}) m_q^2 + c_2 s^2 - c^2}. \end{aligned} \tag{37}$$

Here $m_q, q = 1, 2, 4$ are roots of the equation obtained by equating to zero the determinant of Eq. (15) after ignoring third and fifth rows and columns. Eq. (35) has been solved and discussed in detail by Sharma and Singh [21] for transversely isotropic half-space.

6.3. Stress free elastic half-space

In the absence of piezoelectric, pyroelectric and thermal effects, the various secular equations take the form

$$D^*_{11}D^*_{22} - D^*_{21}D^*_{12} = 0, \tag{38}$$

where

$$\begin{aligned} D^*_{1q} &= (c_3 - c_2) \sin \theta + c_1 m_q V''_q, & D^*_{2q} &= c_2(m_q + \sin \theta V''_q), & q &= 1, 2, \\ V''_q &= -\frac{c_3 m_q s}{c_1 m_q^2 + c_2 s^2 - c^2} = -\frac{c_2 m_q^2 + s^2 - c^2}{c_3 m_q s}, & q &= 1, 2. \end{aligned} \tag{39}$$

Here the roots m_1 and m_2 are given by

$$m_1^2 + m_2^2 = \frac{-(Ps^2 - Jc^2)}{c_1 c_2}, \quad m_1^2 m_2^2 = \frac{(s^2 - c^2)(c_2 s^2 - c^2)}{c_1 c_2}. \tag{40}$$

Eqs. (35) and (38) have also been obtained by Sharma et al. [33] for transversely isotropic plate and in case of isotropic materials by Sharma [34].

7. Numerical results and discussion

The material chosen for the purpose of numerical calculations is CdSe (6 mm class) of hexagonal symmetry, which is transversely isotropic material. The physical data for a single crystal of CdSe material is given below:

$$\begin{aligned} c_{11} &= 7.41 \times 10^{10} \text{ N m}^{-2}, & c_{12} &= 4.52 \times 10^{10} \text{ N m}^{-2}, & c_{13} &= 3.93 \times 10^{10} \text{ N m}^{-2}, \\ c_{33} &= 8.36 \times 10^{10} \text{ N m}^{-2}, & c_{44} &= 1.32 \times 10^{10} \text{ N m}^{-2}, & \beta_1 &= 0.621 \times 10^6 \text{ N K}^{-1} \text{ m}^{-2}, \\ \beta_3 &= 0.551 \times 10^6 \text{ N K}^{-1} \text{ m}^{-2}, & e_{13} &= -0.160 \text{ C m}^{-2}, & e_{33} &= 0.347 \text{ C m}^{-2}, & e_{51} &= -0.138 \text{ C m}^{-2}, \\ \epsilon_{11} &= 8.26 \times 10^{-11} \text{ C}^2 \text{ N}^{-1} \text{ m}^{-2}, & \epsilon_{33} &= 9.03 \times 10^{-11} \text{ C}^2 \text{ N}^{-1} \text{ m}^{-2}, & C_e &= 260 \text{ J kg}^{-1} \text{ K}^{-1}, \\ p_3 &= -2.94 \times 10^{-6} \text{ C K}^{-1} \text{ m}^{-2}, & Y_r &= 4.48 \times 10^{10} \text{ N m}^{-2}, & \alpha_r &= 4.4 \times 10^{-6} \text{ K}^{-1}, \\ \alpha_1 &= 3.92 \times 10^{-12} \text{ C N}^{-1}, & K_1 &= K_3 = 9 \text{ W m}^{-1} \text{ K}^{-1}, & \rho &= 5504 \text{ kg m}^{-3}, & T_0 &= 298 \text{ K}. \end{aligned}$$

The roots m_i , $i = 1, 2, 3, \dots, 8$ of the biquadratic equation (16) have been obtained numerically by using Descartes' procedure, which are then used in various subsequent relevant relations and secular equations. The secular equations (22), (26), (31) and (32) are solved by iteration method to obtain the phase velocity of wave propagation. The phase velocity ($V/\sqrt{c_2}$) profiles in different directions of wave propagation for an electrically shorted/charge free, isothermal/thermally insulated stress free surface of half-space for various values of non-dimensional wavenumber (R) have been obtained. The velocity profiles for piezothermoelastic half-space subjected to various boundary conditions are given in Figs. 2–5. The attenuation coefficient for the wave propagation has also been computed and represented in Figs. 6–9. In order to see the effect of thermal and pyroelectric fields on velocity and attenuation in Rayleigh wave, the corresponding quantities are also computed and shown graphically for piezoelectric elastic half-space. These quantities are plotted in Figs. 10–13.

The variation of non-dimensional phase velocity with wavenumber for charge free isothermal and thermally insulated surface of the half-space is shown in Figs. 2 and 3, respectively. From these figures it is clear that the phase velocity curves are dispersive only for small values of wavenumber in the range $0 \leq R \leq 2$, but for higher values of wavenumber ($R > 2$), these become almost non-dispersive. The magnitude of Rayleigh wave velocity is observed to be higher in thermally insulated case than that of isothermal one. The directional dependence of velocity is also clear from Figs. 2 and 3, which shows that phase velocity increases as wave normal inclination progresses from the axis of symmetry to the free surface which has maximum value for $\theta = 90^\circ$ and minimum value along $\theta = 15^\circ$. Thus the Rayleigh wave velocity is maximum when wave propagates along the free surface and minimum when it travels perpendicular to free surface of the half-space. Figs. 4 and 5 represent the variation in phase velocity for electrically shorted (isothermal and thermally insulated) surface of the half-space. For isothermal case the trend of variations is not similar in all directions of propagation. For the directions close to the x_3 -axis

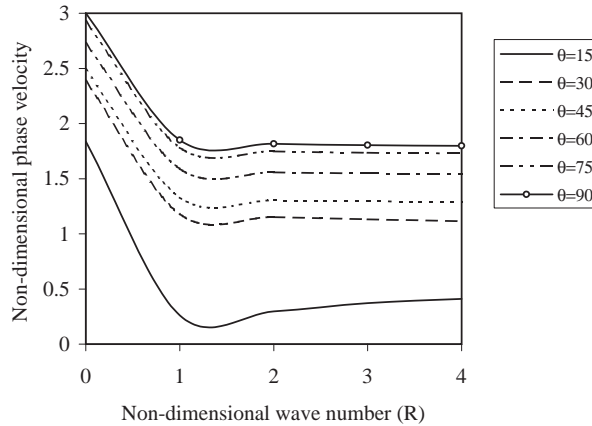


Fig. 2. Variation of phase velocity with wavenumber in various directions (charge free and isothermal boundary conditions).

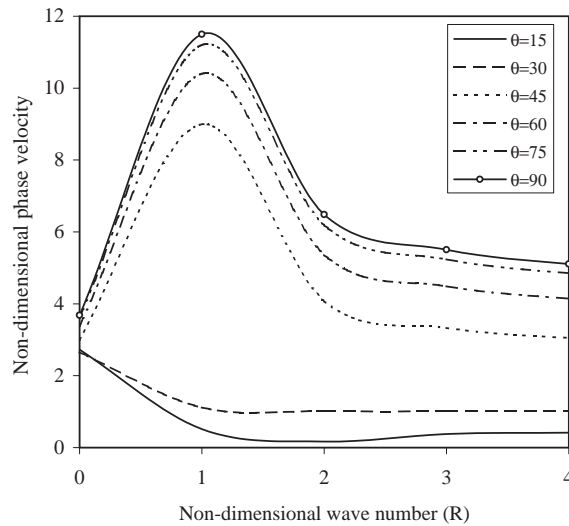


Fig. 3. Variation of phase velocity with wavenumber in various directions (charge free, thermally boundary conditions).

($\theta = 15^\circ, 30^\circ, 45^\circ$) the phase velocity has maximum value at zero wavenumber, which then decreases to attain asymptotically linear value at higher values of the wavenumber. Along other directions phase velocity increases in the interval $0 \leq R \leq 2$ and then the variation becomes linear. There are cross over points for various dispersion curves in different directions in the region $0.5 \leq R \leq 1.0$. When the surface of half-space is thermally insulated, the phase velocity decreases from its maximum value at small values of wavenumber to attain the constant value at higher values of wavenumber. The trend of variation is almost same in all directions.

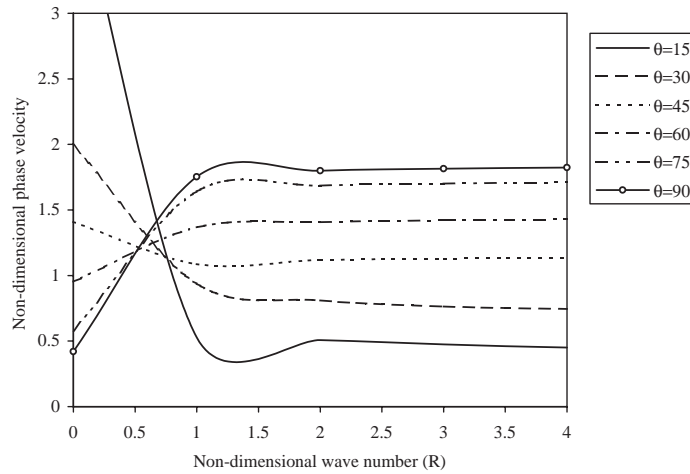


Fig. 4. Variation of phase velocity with wavenumber in various directions (electrically shorted and isothermal boundary conditions).

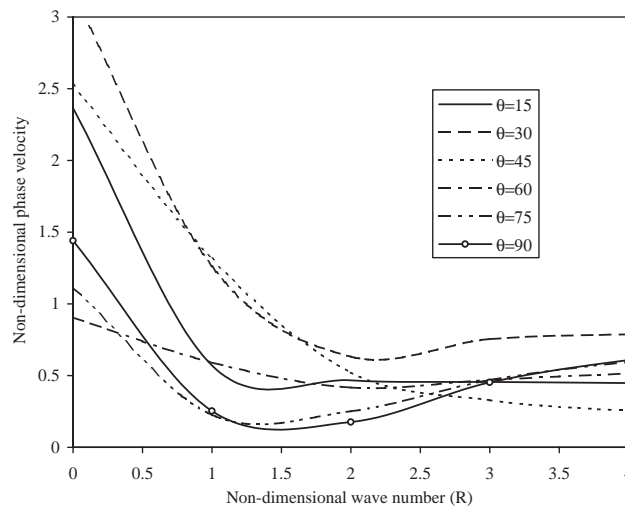


Fig. 5. Variation of phase velocity with wavenumber in various directions (electrically shorted and thermally insulated boundary conditions).

The attenuation of Rayleigh wave propagating in piezothermoelastic half-space is shown in Figs. 6–9 for different boundary conditions at the surface. The variation in attenuation coefficient (Q) with wavenumber for charge-free (isothermal and thermally insulated) surface of the half-space is shown in Figs. 6 and 7, respectively, whereas this quantity for electrically shorted (isothermal and thermally insulated) surface of the half-space is plotted in Figs. 8 and 9, respectively. The magnitude of attenuation coefficient along $\theta = 15^\circ$ is taken one-tenth of the original one in the plot of Figs. 6 and 7 for better clarity. From all these curves it is clear that

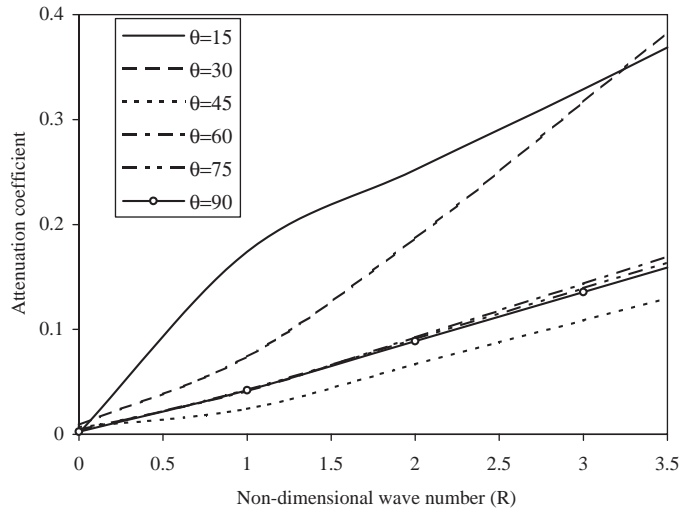


Fig. 6. Variation of attenuation coefficient with wavenumber in various directions (charge free and isothermal boundary conditions).

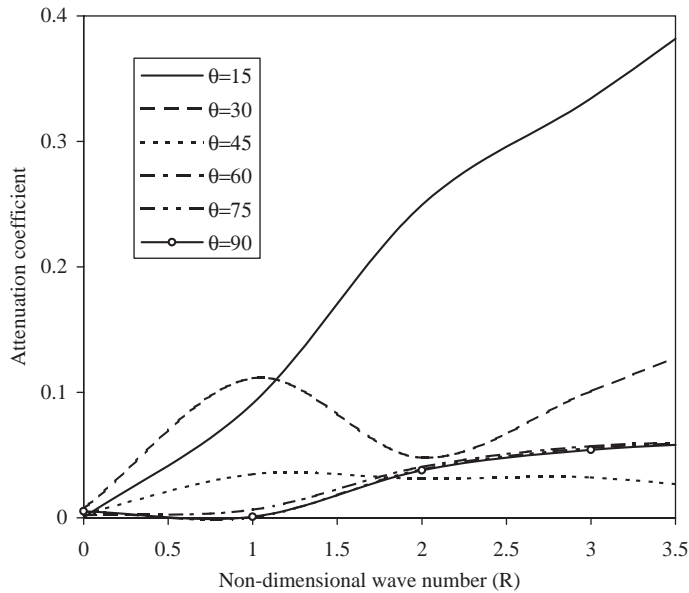


Fig. 7. Variation of attenuation coefficient with wavenumber in various directions (charge free, thermally insulated boundary conditions).

attenuation is maximum along the direction $\theta = 15^\circ$ and least along $\theta = 90^\circ$. Hence there will be more dissipation of energy when the wave penetrate inside the medium than that when it propagate along the surface. This result is also in agreement with the phase velocity profiles where velocity is more along the directions close to the surface and small along the directions near to

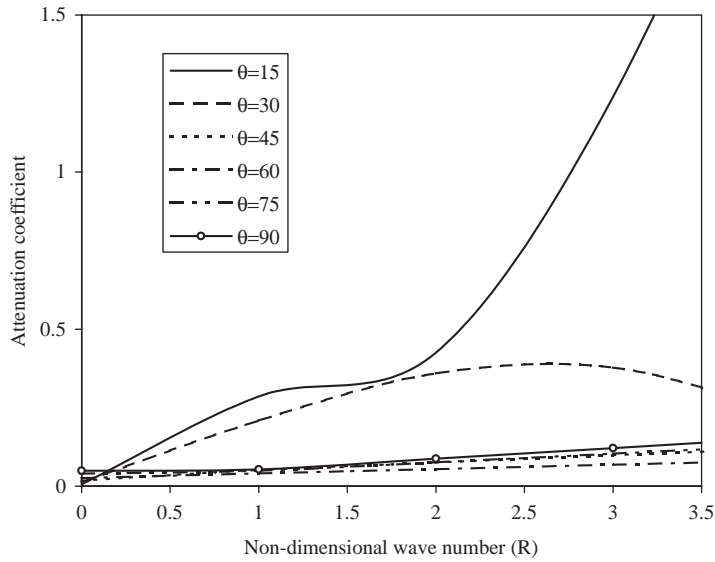


Fig. 8. Variation of attenuation coefficient with wavenumber in various directions (electrically shorted and isothermal boundary conditions).

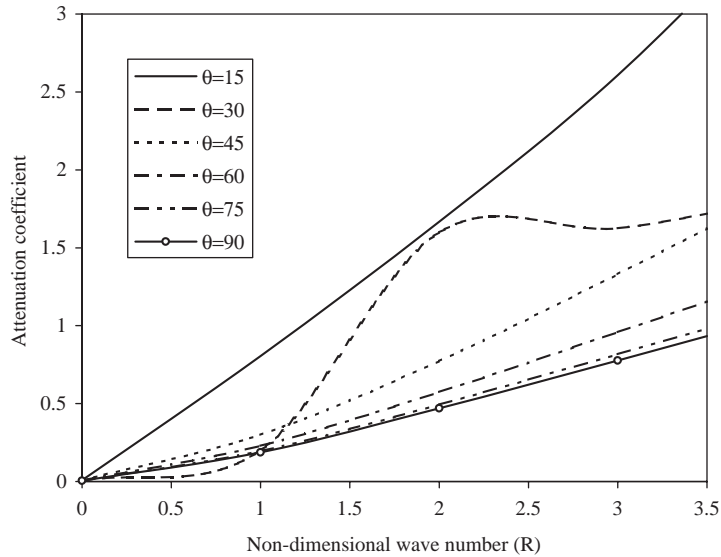


Fig. 9. Variation of attenuation coefficient with wavenumber in various directions (electrically shorted and thermally insulated boundary conditions).

x_3 -axis. For the directions other than $\theta = 15^\circ$, the attenuation is very very small for all the situations discussed except when the surface of half-space is electrically shorted and thermally insulated. In this case significant attenuation is observed in all the directions. It means that all the

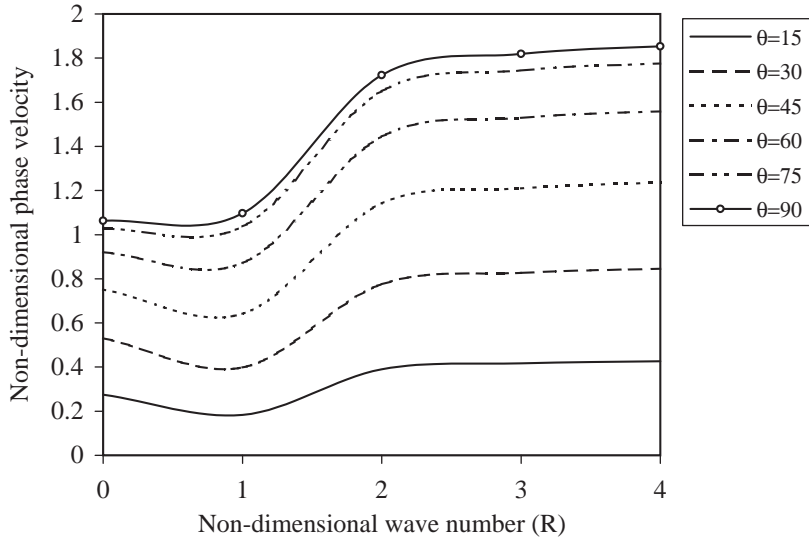


Fig. 10. Variation of phase velocity with wavenumber in various directions in charge free piezoelectric half-space.

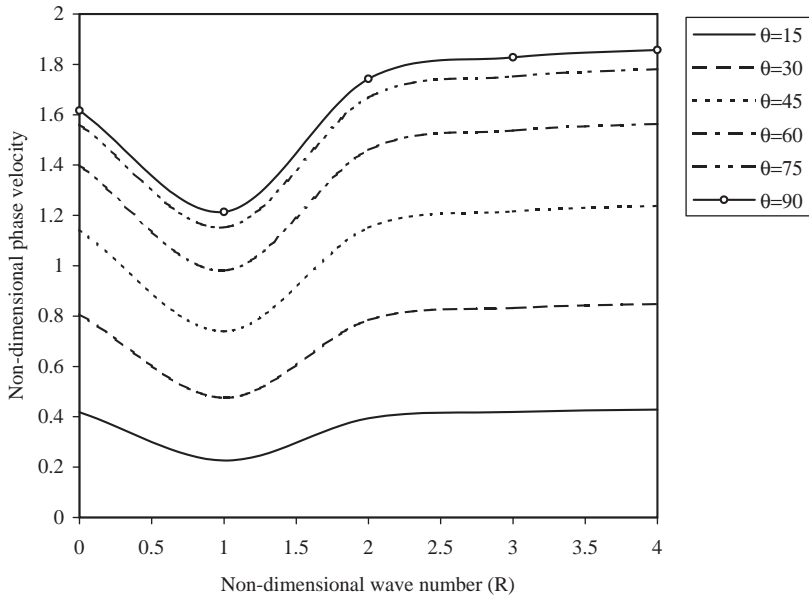


Fig. 11. Variation of phase velocity with wavenumber in various directions in electrically shorted piezoelectric half-space.

fields namely elastic, thermal and electric are coupled strongly with each other in such a situation. Some more curves has been obtained to see the variation of attenuation coefficient with wavenumber in the range $\theta = 15^\circ$ to 30° . These curves are shown in Figs. 14a–d for charge free

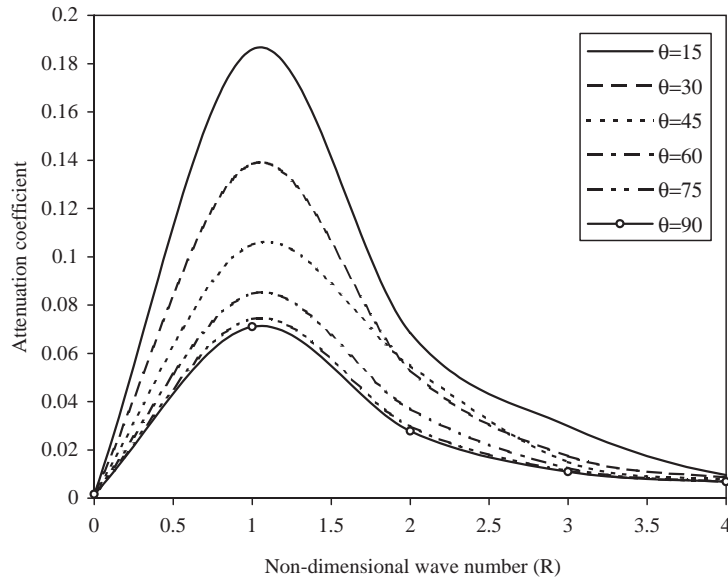


Fig. 12. Variation of attenuation coefficient with non-dimensional wavenumber in various Directions for charge free surface of piezoelectric half-space.

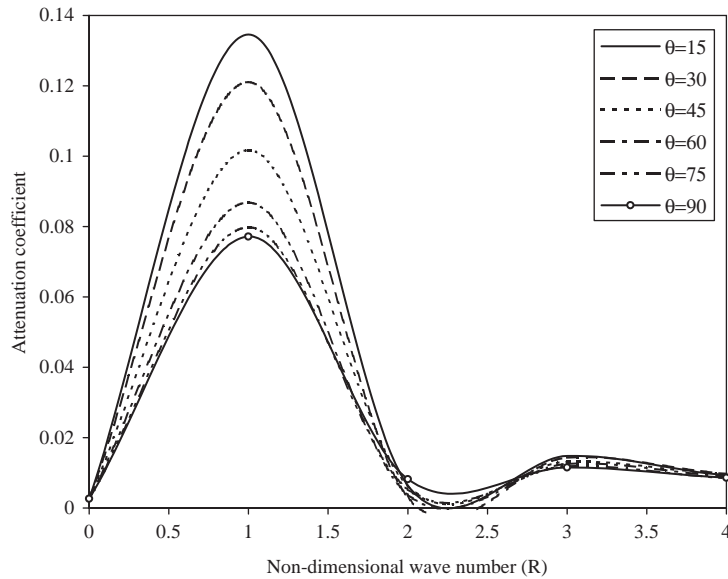


Fig. 13. Variation of attenuation coefficient with non-dimensional wavenumber in various directions for electrically shorted surface of piezoelectric half-space.

and electrically shorted boundaries of the plate, respectively. In case of charge free plate the attenuation coefficient is observed to have minimum value along the direction $\theta = 20^\circ$, the corresponding curve not shown in Fig. 14a but its magnitude is about one-hundredth to that along other directions.

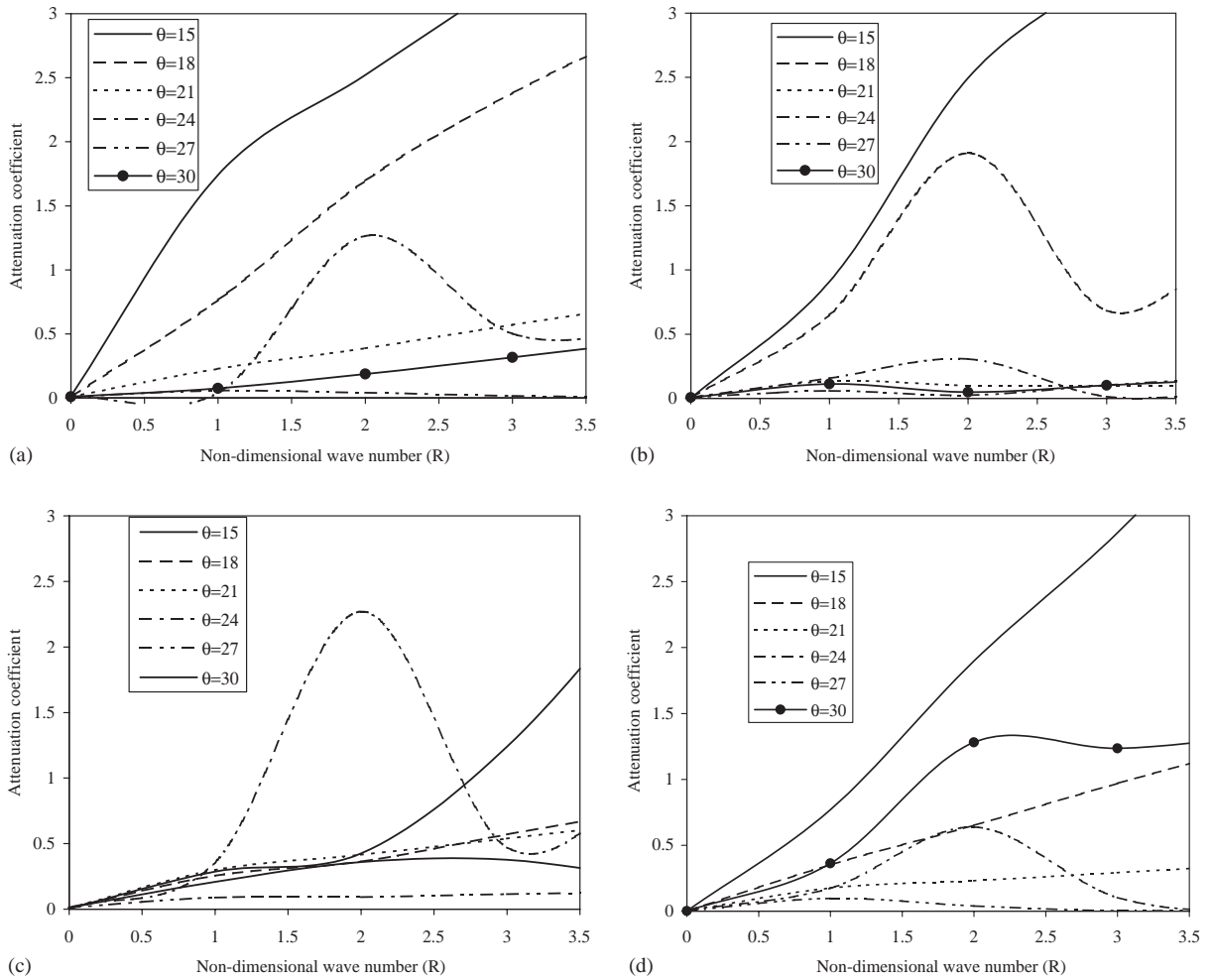


Fig. 14. (a) Variation of attenuation coefficient with wavenumber in various directions ($\theta = 15^\circ, 18^\circ, 21^\circ, 24^\circ, 27^\circ, 30^\circ$) (charge free and isothermal boundaries). (b) Variation of attenuation coefficient with wavenumber in various directions ($\theta = 15^\circ, 18^\circ, 21^\circ, 24^\circ, 27^\circ, 30^\circ$) (charge free and thermally insulated boundaries). (c) Variation of attenuation coefficient with wavenumber in various directions ($\theta = 15^\circ, 18^\circ, 21^\circ, 24^\circ, 27^\circ, 30^\circ$) (electrically shorted and isothermal boundaries). (d) Variation of attenuation coefficient with wavenumber in various directions ($\theta = 15^\circ, 18^\circ, 21^\circ, 24^\circ, 27^\circ, 30^\circ$) (electrically shorted, thermally insulated boundaries).

The phase velocity and attenuation coefficient are also computed for piezoelectric half-space. The variation in phase velocity with wavenumber is shown in Fig. 10 for charge free surface and in Fig. 11 for electrically shorted surface of piezoelectric half-space. The variation in phase velocity is observed to be dispersive in the interval $0 \leq R \leq 2$, whereas at higher values of the wavenumber it is almost linear. It means that half-space behave like a dispersionless medium for higher values of wavenumber. In both the cases the velocity is minimal when the value of non-dimensional wavenumber is unity. Since it is clear from these figures that the velocity is highly dependent on direction of propagation and has maximum value along $\theta = 90^\circ$ and minimum along $\theta = 15^\circ$.

Because velocity is least when the value of non-dimensional wavenumber is unity, so attenuation of wave should be maximal at this range of values of the wavenumber. This fact is quite clear from Figs. 12 and 13, where maximum attenuation is observed when the value of non-dimensional wavenumber is unity. At higher values of wavenumber (> 2) the attenuation is almost negligible. The magnitudes of attenuation coefficient in piezoelectric half-space are very small in magnitude as compared to that in piezothermoelastic half-space. This is due to the fact that dissipation of energy increases with the coupling of thermal and pyroelectric fields with elastic field. Moreover, the comparison of corresponding phase velocity and attenuation profiles for piezothermoelastic and piezoelectric half-space reveals that there is a slight shift of some critical points on the dispersion curves in the former case as compared to the latter one. This establishes the fact that the effect of heat conduction on shift in the frequencies by a small imaginary number thereby signifying the effect of energy dissipation due to heat conduction is to reduce the amplitude of vibrations.

8. Conclusion

The Propagation of Rayleigh waves in a transversely isotropic piezothermoelastic medium subjected to stress free, charge free/electrically shorted and isothermal/thermally insulated boundary conditions at the surface of half-space has been discussed. The secular equations in closed and simple form have been derived. The analysis for elastic, piezoelectric and thermoelastic half-space has been deduced as particular cases from the present one. The variation of phase velocity with non-dimensional wavenumber has been shown graphically for CdSe (6 mm class) material. The velocity profiles are also obtained for piezoelectric half-space in order to observe and note the effect of thermal and pyroelectric fields. In addition to this, attenuation coefficients of waves are also computed and represented graphically with wavenumber. The phase velocity profiles are observed to be dispersive at low values of wavenumber whereas at higher values of wavenumber these have asymptotically linear behaviour. This means that half-space behaves as dispersive medium for Rayleigh wave only for low values of wavenumber. The attenuation is maximal when the wave penetrates deep into the medium and minimum when it propagates along the surface of half-space. The attenuation is more in piezothermoelastic media than that for piezoelectric one. This may be due to coupling of thermal and pyroelectric fields with elastic fields in piezoelectric media. The analytical and numerical results are found to be in close agreement. The results provide evidence that piezoelectric elements can be used effectively as temperature sensors and helps in the construction of intelligent structural systems. This study will be useful in the design and construction of temperature sensors and surface acoustic wave (SAW) filter devices.

Acknowledgements

The authors thankfully acknowledge the financial support from the Council of Scientific and Industrial Research (CSIR), New Delhi via project grants No.25 (0115)/01/EMR-II.

Appendix A

The coefficients a_i , A_i , $i = 1, 2, 3$ in Eq. (16) and $R(m_q)$, $R_i(m_q)$, $i = 1, 2, 3$ in Eq. (18) are given as

$$a_1 = \frac{Ps^2 - Jc^2 + \bar{\epsilon}c_1c_2s^2 + \bar{\epsilon}_\eta[(2c_2e_2 - 2c_3e_1 + e_1^2c_1 + 1)s^2 - c^2]}{c_1c_2 + \bar{\epsilon}_\eta c_2},$$

$$a_2 = \frac{\bar{\epsilon}s^2(Ps^2 - Jc^2) + (s^2 - c^2)(c_2s^2 - c^2) + \bar{\epsilon}_\eta \left[(e_1^2c_2 + e_2^2c_2 - 2c_3e_1e_2)s^4 - e_1^2s^2c^2 + 2e_2s^2(s^2 - c^2) \right]}{c_1c_2 + \bar{\epsilon}_\eta c_2},$$

$$a_3 = \frac{s^2(s^2 - c^2)[\bar{\epsilon}(c_2s^2 - c^2) + \bar{\epsilon}_\eta e_2^2s^2]}{c_1c_2 + \bar{\epsilon}_\eta c_2},$$

$$A_1 = \frac{\{E_1(P's^2 - J'\bar{c}^2) + \bar{\epsilon}C_1C_2s^2 + \bar{\epsilon}_\eta[(2C_2\bar{e}_2 - (E+1)\bar{e}_1C_3 + \bar{e}_1^2C_1 + E^2)s^2 - E^2\bar{c}^2]\}}{C_1C_2E_1 + \bar{\epsilon}_\eta E^2C_2},$$

$$A_2 = \frac{\left\{ \begin{array}{l} \bar{\epsilon}s^2(P's^2 - J'\bar{c}^2) + E_1(s^2 - \bar{c}^2)(C_2s^2 - \bar{c}^2) \\ + \bar{\epsilon}_\eta[(\bar{e}_1^2C_2 + \bar{e}_2^2C_2 - 2C_3\bar{e}_1\bar{e}_2)s^4 + 2E\bar{e}_2(s^2 - \bar{c}^2)s^2 - \bar{e}_1^2s^2\bar{c}^2] \end{array} \right\}}{C_1C_2E_1 + \bar{\epsilon}_\eta E^2C_2},$$

$$A_3 = \frac{s^2(s^2 - \bar{c}^2)[\bar{\epsilon}_\eta\bar{e}_2^2s^2 + \bar{\epsilon}(C_2s^2 - \bar{c}^2)]}{C_1C_2E_1 + \bar{\epsilon}_\eta E^2C_2},$$

$$R(m_q) = -\epsilon_{ps} \left\{ \begin{array}{l} [c_3(\bar{\beta}\bar{\epsilon}_\eta - p) + (\bar{\beta} + pc_1)e_1 - c_1\bar{\epsilon}_\eta - 1]m_q^4 + \\ [c_3(\bar{\beta}\bar{\epsilon}_\eta\bar{\epsilon} - pe_2) + e_1(pc_2 + \bar{\beta}e_2) - 2e_2 - \bar{\epsilon}_\eta(\bar{\epsilon}c_1 + c_2)s^2 - (pe_1 - \bar{\epsilon}_\eta)c^2]m_q^2 \\ - s^2[(\bar{\epsilon}_\eta\bar{\epsilon}c_2 + e_2^2)s^2 - \bar{\epsilon}_\eta\bar{\epsilon}c^2] \end{array} \right\},$$

$$R_1(m_q) = \epsilon_{pm_q} \left\{ \begin{array}{l} c_2(\bar{\beta}\bar{\epsilon}_\eta - p)m_q^4 + \\ \{[\bar{\beta}\bar{\epsilon}_\eta(\bar{\epsilon}c_2 + 1) + e_1^2\bar{\beta} - p(1 + c_2e_2 - c_3e_1) - (\bar{\epsilon}_\eta c_3 + e_1)]s^2 - (\bar{\beta}\bar{\epsilon}_\eta - p)c^2\}m_q^2 \\ + s^2[(s^2 - c^2)(\bar{\beta}\bar{\epsilon}_\eta\bar{\epsilon} - pe_2) - (c_3\bar{\epsilon}_\eta\bar{\epsilon} + e_1e_2)s^2] \end{array} \right\},$$

$$R_2(m_q) = m_q \left\{ \begin{array}{l} (pc_1 + \bar{\beta})c_2m_q^4 + [p(Ps^2 - Jc^2) + \bar{\beta}(s^2 - c^2) + (e_1c_1 - c_3 + \bar{\beta}e_2c_2 - \bar{\beta}c_3e_1)s^2]m_q^2 \\ + (s^2 - c^2)[(pc_2 + \bar{\beta}e_2)s^2 - pc^2] + (e_1c_2 - c_3e_2)s^4 - e_1c^2s^2 \end{array} \right\},$$

$$R_3(m_q) = \epsilon_P \left\{ \begin{aligned} & c_2(1 + \bar{\epsilon}_\eta c_1)m^6 + \left[-\{c_3(c_3\bar{\epsilon}_\eta + e_1) + e_1(c_3 - e_1c_1)\}s^2 + (\bar{\epsilon}c_1 + 1)(s^2 - c^2) \right] m_q^2 \\ & + \left[\{-c_3(c_3\bar{\epsilon}_\eta\bar{\epsilon} + e_1e_2) + e_1(e_1c_2 - e_2c_3)\}s^4 + c_2s^2\{\bar{\epsilon}_\eta\bar{\epsilon}(c_2s^2 - c^2) + e_2^2s^2\} \right] m_q^2 \\ & \quad + (s^2 - c^2)\{c_1\bar{\epsilon}_\eta\bar{\epsilon} + c_2\bar{\epsilon}_\eta + 2e_2\}s^2 - \bar{\epsilon}_\eta c^2 \\ & \quad + (s^2 - c^2)s^2\{\bar{\epsilon}_\eta\bar{\epsilon}(c_2s^2 - c^2) + e_2^2s^2\} \end{aligned} \right\},$$

where

$$C_1 = \frac{(c_1 + \epsilon \bar{\beta}^2)}{1 + \epsilon}, \quad C_2 = \frac{c_2}{1 + \epsilon}, \quad C_3 = \frac{c_3 + \epsilon \bar{\beta}}{1 + \epsilon}, \quad \bar{e}_1 = \frac{e_1 - \epsilon p}{1 + \epsilon}, \quad \bar{e}_2 = \frac{e_2}{1 + \epsilon},$$

$$E = \frac{(1 - \epsilon \bar{\beta}p)}{1 + \epsilon}, \quad \bar{\epsilon} = \frac{\bar{\epsilon}}{1 + \epsilon}, \quad E_1 = \frac{(1 - \epsilon p^2/\eta_3)}{1 + \epsilon}, \quad \bar{c}^2 = \frac{c^2}{1 + \epsilon},$$

$$P = c_1 + c_2^2 - c_3^2, \quad J = c_1 + c_2, \quad P' = C_1 + C_2^2 - C_3^2, \quad J' = C_1 + C_2,$$

$$F = \frac{(1 + \epsilon)^3 C_2 (C_1 E_1 + \bar{\epsilon}_\eta E^2)}{c_2 (c_1 + \bar{\epsilon}_\eta)}.$$

References

- [1] R.D. Mindlin, On the equations of motion of piezoelectric crystals, problems of continuum, in: N.I. Muskhelishvili (Ed.), *Mechanics*, 70th Birthday Volume, SIAM, Philadelphia, 1961, pp. 282–290.
- [2] R.D. Mindlin, *Equation of High Frequency Vibrations of Thermo-piezoelectric, Crystal Plates, Interactions in Elastic Solids*, Springer, Wein, 1979.
- [3] W. Nowacki, Some general theorems of thermo-piezoelectricity, *Journal of Thermal Stresses* 1 (1978) 171–182.
- [4] W. Nowacki, Foundations of linear piezoelectricity, in: H. Parkus (Ed.), *Electromagnetic Interactions in Elastic Solids*, Springer, Wein, 1979 (Chapter 1).
- [5] W. Nowacki, New problems in mechanics of continua, *Mathematical Modes of Phenomenological Piezoelectricity*, University of Waterloo Press, Ontario, 1983, pp. 29–49.
- [6] D.S. Chandrasekharaiah, A temperature rate dependent theory of piezoelectricity, *Journal of Thermal Stresses* 7 (1984) 293–306.
- [7] D.S. Chandrasekharaiah, A generalized linear thermoelasticity theory of piezoelectric media, *Acta Mechanica* 71 (1988) 39–49.
- [8] A.K. Pal, Surface waves in a thermo-piezoelectric medium of monoclinic symmetry, *Czechoslovak Journal of Physics* 29 (1979) 1271–1281.
- [9] A.P. Mayer, Thermoelastic attenuation of surface acoustic waves, *International Journal of Engineering Sciences* 28 (1990) 1073–1082.
- [10] H.S. Paul, K. Ranganatham, Free vibrations of a pyroelectric layer of hexagonal (6mm) class, *Journal of the Acoustical Society of America* 78 (1985) 395–397.
- [11] P. Chadwick, L.T.C. Seet, Wave propagation in transversely isotropic heat conducting elastic materials, *Mathematica* 17 (1970) 255–274.
- [12] P. Chadwick, Basic properties of plane harmonic waves in prestressed heat conducting elastic material, *Journal of Thermal Stresses* 2 (1979) 193–214.

- [13] J.N. Sharma, R.S. Sidhu, On the propagation of plane harmonic waves in anisotropic generalized thermoelasticity, *International Journal of Engineering Science* 24 (1986) 1511–1516.
- [14] H. Singh, J.N. Sharma, Generalized thermoelastic waves in transversely isotropic media, *Journal of the Acoustical Society of America* 77 (1985) 1046–1053.
- [15] J.N. Sharma, On the low and high frequency behaviour of generalized thermoelastic waves, *Archives of Mechanics* 38 (1986) 665–673.
- [16] J.N. Sharma, V. Kumar, S.P. Sud, Plane Harmonic waves in orthotropic thermoelastic materials, *Journal of the Acoustical Society of America* 107 (2000) 293–305.
- [17] P. Chadwick, in: R. Hill, I.N. Sneddon (Eds.), *Progress in Solid Mechanics*, Vol. 1, North-Holland, Amsterdam, 1960.
- [18] A. Nayfeh, S.N. Nasser, Thermoelastic waves in solids with thermal relaxation, *Acta Mechanica* 12 (1971) 53–69.
- [19] P. Chadwick, D.W. Windle, Propagation of Rayleigh isothermal and insulated boundaries, *Proceedings of the Royal Society of America* 280 (1964) 47–71.
- [20] P. Chadwick, R.J. Atkin, Surface waves in heat conducting elastic body-correction and extension of paper of Chadwick and Windle, *Journal of Thermal Stresses* 4 (1981) 509–521.
- [21] J.N. Sharma, H. Singh, Thermoelastic surface waves in a transversely isotropic half space with thermal relaxation, *Indian Journal of Pure and Applied Mathematics* 16 (1985) 1202–1219.
- [22] J.S. Yang, R.C. Batra, Free vibrations of a linear thermo-piezoelectric body, *Journal of Thermal Stresses* 18 (1995) 247–262.
- [23] J.N. Sharma, M. Kumar, Plane harmonic waves in piezo-thermoelastic materials, *Indian Journal of Engineering and Material Science* 7 (2000) 434–442.
- [24] J.N. Sharma, M. Pal, Propagation of Lamb waves in transversely isotropic piezoelectric elastic plate, *Indian Journal of Engineering and Material Science* 10 (2003).
- [25] J.N. Sharma, M. Pal, Rayleigh Lamb waves in magneto-thermoelastic homogeneous isotropic plate, *International Journal of Engineering Science* 42 (2004) 137–155.
- [26] K.F. Graff, *Wave motion in Elastic Solids*, Dover, New York, 1991.
- [27] J.D. Achanbach, *Wave motion in Elastic Solids*, North-Holland, Amsterdam, 1973.
- [28] L. Rayleigh, On waves propagating along the plane surface of an elastic solid, *Proceedings of the London Mathematical Society* 17 (1885) 4.
- [29] R. Stoneley, *Monthly Notices of Royal Astronomical Society Geophysics* 5 (Suppl) (1949) 343.
- [30] V.P. Buchwald, Rayleigh waves in transversely isotropic media, *Quarterly Journal of Mechanics and Applied Mathematics* 14 (1961) 293–304.
- [31] A.M.Abd. Alla, Propagation of Rayleigh waves in an elastic half space of orthotropic material, *Applied Mathematics and Computation* 99 (1999) 61–69.
- [32] J.L. Synge, Elastic waves in anisotropic media, *Journal of Mathematical Physics* 41 (1957) 323–334.
- [33] J.N. Sharma, Devinder Singh, Rajneesh Kumar, Generalized thermoelastic waves in transversely isotropic plates, *Indian Journal of Pure and Applied Mathematics* 34 (2003) 841–852.
- [34] J.N. Sharma, On the propagation of thermoelastic waves in homogeneous isotropic plates, *Indian Journal of Pure and Applied Mathematics* 32 (2001) 1329–1341.